Hydrogeology Journal - Electronic Supplementary Material

Rethinking groundwater flow on the South Rim of the Grand Canyon, USA: characterizing recharge sources and flow paths with environmental tracers

John E. Solder*, Kimberly R. Beisner, Jessica Anderson, Don J. Bills

*Corresponding author: jsolder@usgs.gov, U.S. Geological Survey, Utah Water Science Center, 2329 W. Orton Cir, SLC UT 84119, orcid: 0000-0002-0660-3326

1. Tracer Systematics, Sample Collection, and Analytical Methods

Noble gases are naturally present in the atmosphere and incorporated into groundwater during recharge. The equilibrium concentration of noble gases dissolved in recharging groundwater is a function of barometric pressure, water temperature, and salinity following Henry's Law. As each gas has differing solubilities, measured concentrations can be used to inversely solve for the recharge conditions providing useful information about recharge source and processes (Aeschbach-Hertig et al., 2000). Relative abundance of helium (^{3}He, ^{4}He) and neon (^{20}Ne) isotopes in the atmosphere are distinct from terrestrial sources (crust and mantle) such that $^{3}He/^{4}He$ and $^{4}He/^{20}Ne$ in groundwater can be used to track fluid and gas origins (Solomon, 2000). Helium exchange between deep crustal and mantle reservoirs and shallow groundwater can be used to trace fluid sources and has important implications for groundwater chemistry and the South Rim conceptual model. Tritiogenic helium-3 ($^{3}He_{trit}$) is derived from the radio-decay of tritium and is useful age tracer of water recharged after 1950. Tritiogenic helium-

3 can be determined after accounting for other sources of helium if no appreciable mantle source is present (Solomon and Cook, 2000).

Tritium (^{3}H) and ^{14}C are cosmogenic isotopes, also produced in nuclear fission, with half-lives of 12.32 years (Lucas and Unterweger, 2000) and 5,730 years (Kalin, 2000), respectively, making them useful for estimating groundwater age. Above-ground nuclear testing between approximately 1950 and the early 1960s significantly increased atmospheric concentrations of ^{3}H and ^{14}C over the same period. The so-called 'bomb pulse' is readily identified in groundwater samples by tracer concentrations greater than background levels for northern Arizona of ~ 7 tritium units (TU) and 100 percent modern carbon (pmC), respectively (Michel et al., 2018; Reimer et al., 2013). Background ^{3}H decayed to 2016 is ~0.2 TU, a useful criterion for differentiating between modern water recharged post-1950 and pre-modern water recharged pre-1950. ^{3}H is particularly useful as a tracer as it is part of the water molecule and samples are unlikely to be contaminated or affected by reactions other than radioactive decay. ^{14}C is the most commonly used tracer for dating 1,000s to 10,000s year old groundwater, but frequently must be corrected for geochemical and isotopic exchange other than radioactive decay (Han and Plummer, 2013). Further discussion of groundwater age calculation and geochemical correction of ^{14}C can be found in the methods section of the main text.

Most samples were collected from springs and processed following standard protocol (Gibs et al., 2012; Radtke et al., 2002; Ritz and Collins, 2008; Rounds, 2012; Rounds et al., 2013; Skrobialowski, 2016; U.S. Geological Survey, 2006, 2019a; Wilde et al., 2014; Wilde, 2002, 2004, 2006). Well samples collected for this study made use of dedicated submersible pumps. Once samples were collected, processed, and properly preserved they were hiked to a place where they could be stored appropriately until they could be shipped to their respective

labs for analysis. Noble gas water samples were collected by flushing and filling a copper sample tube, in duplicate, with pinch clamp closures (Weiss, 1968). Copper tubes were closed under backpressure and while water was flowing through to limit degassing and back diffusion of gas. Dissolved noble gases were analyzed at the University of Utah Noble Gas Lab. The gases were extracted from the water and cryogenically separated. Heavier gases (Ne, Ar, Kr, Xe) were measured using a quadrupole mass spectrometer. Helium isotopes were measured using a sector-field mass spectrometer. Helium and neon concentrations have an uncertainty of ±1.5%. Argon, krypton, and xenon concentrations have an uncertainty of ± 2%. Other major total dissolved gas components (i.e., O_2, N_2, CH_4, CO_2) were also analyzed from the copper tube samples by quadrupole mass spectrometer. No preservation was attempted for these reactive gases at the time of sampling and are only discussed here as qualitative measures. Stable isotopes of water were collected as part of a companion study—details of stable isotope sample collection, analytical methods, and data interpretation are provided in Solder and Beisner (2020). Alkalinity and ^{14}C water samples were filtered using a 0.45 micron capsule filter. Tritium and stable isotopes were collected as raw samples. ^{3}H samples were processed by distillation and electrolytic enrichment and then analyzed using liquid scintillation counters (Thatcher et al., 1977) at the USGS Menlo Park Tritium Laboratory. ^{14}C samples were collected by overflowing sample water in ground glass stoppered bottles used for low-volume sampling. A copper tube was inserted in the bottom of the sample bottle for overflow. A short section of rubber tubing was used to route sample water from source to bottle. ^{14}C and $\delta^{13}C$ abundances were analyzed by the National Ocean Sciences Accelerator Mass Spectrometry (NOSAMS) Laboratory at the Woods Hole Oceanographic Institution.

2. Tracer Data Interpretation

2.1 Dissolved Noble Gas

The Closed Equilibrium (CE) noble gas solubility model (Aeschbach-Hertig et al., 2000) was used to fit gas concentrations by varying recharge temperature, recharge elevation as a proxy for barometric pressure, excess air, and the fractionation of gases. The CE modeled value of entrapped air (A_e) was converted to excess air (EA) for reporting in this study, which at common water table conditions, have generally similar values (Aeschbach-Hertig et al., 2008). Noble gas temperature (NGT) and recharge elevation are codependent such that the groundwater temperature lapse rate, which matches the adiabatic lapse rate with a small offset, was used to constrain reasonable NGTs and elevations following Manning and Solomon (2003). Groundwater temperatures from within the study area from National Water Information System (USGS, 2019b) were investigated, but there were little data available from shallow groundwater well screen intervals near the water table. Thirty-year mean annual air temperatures (1981-2010) for South Rim weather stations (NOAA, 2018) were used to estimate the temperature lapse rate. A +3 °C correction was added to the lapse rate as a point of common practice given water table temperatures have been observed to be slightly warmer that air temperatures (Manning and Solomon, 2003). The observed and corrected lapse rate define a temperature lapse window and result in estimation of a minimum and maximum for the NGT and recharge elevation. Where the minimum elevation defined by the lapse rate was less than the sample site elevation, the maximum NGT was calculated for the site elevation. The most recent water table elevation reported in NWIS was used to calculate the minimum NGT for Canyon Mine Observation Well. The water table at Havasupai Well is generally shallow (< 20 m) so the land surface elevation

was used. Mixtures of groundwater sources with distinct recharge conditions are not explicitly handled by the CE model. The limited number of noble gases mean the model is under-determined for explicit separation of more than one recharge source. In these cases, the CE modeled NGT and recharge elevation represent a mean value of the recharge captured by the sample.

Sampling and analysis of dissolved gases in South Rim groundwater presented a significant challenge. In general, karstic groundwater systems provide opportunity for degassing of the atmospheric gases prior to discharge if large gas filled void spaces not in equilibrium with the water are encountered (e.g., Han et al., 2017). As with any chemical analysis, the utility of results is contingent on the quality of sample collection. This is particularly true for noble gases in groundwater as noble gases are present in the atmosphere, dissolved concentrations are often in excess of air equilibrated values, and the low solubility of He in particular make the samples very sensitive to contact with the atmosphere or degassing prior to collection. As the goal of noble gas modeling is to capture conditions under which the sample equilibrated with the atmosphere at the time of recharge, correction for re-equilibration of concentrations in unlikely to be successful. Reverse solubility of noble gases with respect to temperature causes an increase in modeled recharge temperatures because gas loss is not accounted for. Dissolved gas re-equilibration with free gas, at a second set of physical conditions not representative of the conditions at recharge, will *reset* the gas signature. Most commonly, gas loss occurs with atmospheric contact at the point of discharge, which can be reasonably mitigated by careful sampling technique and site selection. Gas loss can also occur during 1) exsolution resulting in bubble formation, and 2) exchanged with free gas already present in the system such as gas-filled void spaces. If after re-equilibration, the free gas escapes the system such that a second

different free gas composition exchanges with the water, the CE model results will capture the second set of re-equilibration conditions. The CE model captures the occurrence of gas loss (i.e., $F > 1$, $A_e < 1$; Aeschbach-Hertig et al., 2008) but the original recharge conditions cannot be reconstructed. Of all the samples, multiple gas exchanges were most likely to have occurred at Blue and Cataract Canyon Springs where visible bubbles at the spring source and large tufa deposits, resulting from decreased calcite solubility driven by CO_2 gas loss and increasing pH, were observed. The addition of non-atmospheric gas largely in the form of deeply sourced CO_2 (Crossey et al., 2006) results in a condition where the ratio of the exsolved gas bubble volume to sample water volume at the final state (i.e., point of sampling) is larger than the bubble to water ratio at the initial state (i.e., recharge; Aeschbach-Hertig et al., 2008). Continued exsolution and rapid upward transport of mainly CO_2 bubbles could facilitate multiple exchanges. Despite these factors, measured noble gas concentrations are reasonably captured by the CE model and we feel the interpretive results advance the study's goals. Knowledge of the sample collection and site conditions was used to critically evaluate the model results. Future use of the dissolved gas data collected as part of this study should consider these limitations.

2.2 Helium Isotopes

Relative abundances of stable isotopes of helium (^{3}He and ^{4}He) for terrestrial sources (atmosphere, crust, and mantle) are distinct such that measured helium isotopes in groundwater can be used to track fluid and gas origins (Solomon, 2000). Isotopic helium ratios (R; ^{3}He/^{4}He) are reported relative to the relatively constant ratio in the atmosphere (R_a; 1.384×10^{-6}). By this convention AEW has an R/R_a value of 1. Crustal helium sourced from U and Th series decay has a R/R_a between 0.02 and 0.3 (Mamyrin and Tolstikhin, 1984; Andrews, 1985). Sub-continental

lithospheric mantle (SCLM) helium from radioactive decay and primordial sources has a R/R_a ~6 (Gautheron and Moreira, 2002), while the bulk mantle has R/R_a ~8 as approximated by helium trapped in mid-ocean ridge basalts (MORB). Based on the differences in isotopic ratios, a helium mass balance can be calculated to determine the individual contributions of helium from the atmosphere, crust, mantle, and decay of ^3H ($^3He_{trit}$; Solomon, 2000; Kulongski and Hilton, 2011). In samples with a significant mantle He component, the contribution of He_{trit} cannot be reliably estimated, the implications of which are discussed later.

In shallow groundwater, atmospheric He from solubility equilibrium and excess air is commonly the largest component of the helium budget. The remaining He (excluding $^3He_{trit}$) sourced from crust and mantle is referred to as terrigenic helium (He_{terr}). The relative contribution of He_{terr} can be quantified by the ratio of ^4He to ^{20}Ne (Ballentine et al., 1991). As there is no meaningful source of ^{20}Ne other than the atmosphere, measured ratios of $^4He/^{20}Ne$ that deviate from the atmospheric ratio of 0.288 are likely contain He_{terr}. Samples with measured ratios of $^4He/^{20}Ne$ much greater than 0.288 (i.e., 10 times greater) contain a negligible amount of atmospheric helium. For samples in which the crust and mantle components of the helium budget are dominant, helium isotope ratios corrected for the atmospheric contributions (i.e., R_c/R_a) will not significantly differ from measured R/R_a. A plot of R/R_a versus $^4He/^{20}Ne$ was used to identify dissolved helium sources (Fig. 4 of main text).

For samples dominated by terrigenic source of helium, the fraction of helium derived from mantle (F_{SCLM}) versus the crust can then be determined by binary mixing model as:

$$F_{\mathrm{SCLM}} = \frac{\frac{R}{R_a}\ \text{of sample} + \frac{R}{R_a}\ \text{of crust}}{\frac{R}{R_a}\ \text{of crust} + \frac{R}{R_a}\ \text{of mantle}} \qquad \text{(S1)}$$

For this study, R/R_a of the crust was assumed to range between 0.02 and 0.15, and R/R_a of the SCLM was assumed to be 6. The estimate of F_{SCLM} provides some quantification of mantle He but is not a measure of the fraction of water which was in contact with the mantle. Deeply sourced gases, particularly the relatively light and insoluble He isotopes, can easily travel through the substrata and water column as bubbles and thorough diffusion without any actual advection of water between the two reservoirs. In the above calculations for determining helium source components it is assumed that no fractionation of He isotopes, with the exception of the initial exchange between the atmosphere and infiltrating water, has taken place.

2.3 Groundwater Age

2.3.1 Interpretation Method

Although the conceptual model of recharge sources provides important insights and guides LPM interpretations, simplified LPMs were selected for many of the sites because multiple tracers were not available. More complex LPMs that may better represent the physical complexity of recharge sources and the groundwater flow-system require a larger number of fitting parameters and thus were under-determined with the data available in this study. A conservative approach was taken of using simplified LPMs except where tracer data was incongruent, and all available tracer concentrations for a given site could not be adequately reconciled using an LPM.

Conceptually, the exponential piston-flow model (EPM; Jurgens et al., 2012) is an appropriate starting place for constraining South Rim LPMs. The EPM describes an aquifer where areally uniform recharge (i.e., exponential model) occurs over a discrete area at the

upgradient extent of the aquifer, and flow paths become confined, approximating a piston-flow model (PFM), as water moves down gradient toward the discharge point. The fitting parameter for the EPM is the ratio of the confined length to the unconfined length of the flow path (Jurgens et al., 2012). In South Rim aquifers, the confinement can be either physical (e.g., recharge is physically prevented by a confining unit), hydrological (e.g., limited recharge occurs over the piston-flow portion of the flow path length), or both. EPM ratios were estimated based on hypothetical flow paths between the presumed primary recharge area (San Francisco Peaks) and the respective groundwater sampling site. The length of the recharge zone flow path was varied, with the transition from unconfined to confined flow varied between from the base of the San Francisco Peaks to the outer extent of elevation greater than ~2,000 m relative to North American Vertical Datum of 1988 (Fig. 1 of main text), to provide some estimation of uncertainty in the EPM ratio. Although later results of this study bring the EPM conceptual model into question for some sites, it is a good starting point for the investigation of groundwater age and almost certainly provides a better representation than a piston-flow only approximation (i.e., apparent tracer age).

For tracer concentrations best fit by the extreme end-members of the EPM (i.e., either a very small or very large EPM ratio) simplified LPMs were adopted. The dispersion model (DM) with a dispersion parameter of 0.01, representing longitudinal dispersive mixing along km scale flow paths (Gelhar et al., 1992), was used to approximate samples approaching a piston-flow (PFM) age distribution which assumes no mixing. The exponential mixing model (EMM) was used to approximate samples where the confined length was very small and assumes that groundwater recharge is equal across the capture area. For select sites where observed tracer data cannot be explained by a single recharge source, a binary mixing model (BMM) is employed.

Conceptual diagrams and further explanation of the LPMs is provided by Jurgens et al. (2012) and references therein. Based on the number of assumptions required to fit LPMs to the observed tracer data, confidence in representativeness of the true age distribution is generally low. As such, only mean ages are presented here.

Minimum BMM parameters include the age of the young and old component and the mixing fraction which requires at least three reliable tracer concentrations. Due to the limited tracer availability, BMMs are poorly constrained and are used sparingly. The old component mean age was estimated based on near-by samples expected to be representative of the deep regional groundwater flow system. The remaining young fraction mean age and mixing fraction are then optimized based on the observed tracers for that given site.

A tracer-tracer plot (Jurgens et al., 2012) of ^{3}H versus ^{14}C was used to identify samples that could not be reasonably explained by a single distribution of groundwater ages (Fig. S1). Groundwater tracer concentrations (points) are plotted against modeled age distributions represented by the continuous functions of tracer concentrations with respect to age, i.e., a discrete position on the line corresponds to a specific mean age. The modeled age distributions are a function of sampling date, so the plot shown here is meant for illustrative purposes. Sample date specific cross-plots were reviewed during LPM selection for each sample. The dispersion model with a parameter of 0.01 (DM; limited mixing of flow-paths similar to piston-flow) and exponential mixing model (EMM; complete mixing of flow-paths) bound the region where the groundwater data can be reasonably represented by a single age distribution (Fig. S1). The second lower bounded region defines the possible tracer combinations best explained using a binary mixture model (BMM) of two separate age distributions, conceptually representing contributions from separate and distinct recharge sources. Fitting parameters for respective

LPMs within each region were optimized to match the available tracer data and, in some cases, estimated based on physical aquifer dimensions. For BMMs, the old component of the mixture was estimated from optimized LPM parameters from nearby sites. For data points that fall above the bounded region (^{14}C > ~100 pmC), adjusted ^{14}C is over-predicted or the sample is largely composed of modern water where the adjusted ^{14}C could be consistent with the measured ^{3}H but is too uncertain for age dating. In these cases, estimated mean ages were assigned using ^{3}H alone.

2.3.2 Results

A single LPM (i.e., not a binary mixture) was selected to estimate mean age for 55 samples and the remaining samples (n = 15) were fit by BMMs (Table S1 of the electronic supplementary material ESM2). Of single LPMs, the EPM was selected most frequently (n = 39) with estimated EPM ratios varying between 0.004 and 5 with a mean value of ~1. The EMM and DM were used to estimate mean age for 13 and 3 samples, respectively. BMM distributions were estimated to be a mixture of two EPMs which allowed for the flexibility of the young component of the mixture to vary between the DM and EMM. In most cases, the BMM was under-defined (too few tracers to unique define all LPM parameters) but tracer data could not otherwise be reconciled. LPM parameters for the old component of the BMMs was estimated from LPM fits to samples likely to represent the deep regional groundwater flow in the Redwall-Muav aquifer. Depending on the hydrologic position of the sample site, Bar Four or Canyon Mine Observation Wells, or Indian Garden Spring LPMs were used to estimate the age distribution of the old fraction age in BMMs (Table S1 of the ESM2). Uncertainty in mean age resulting from uncertainties in estimated LPM parameters (rather than fit using multiple tracers) was quantified by estimating mean ages for two sets of LPM parameters for each site. This is not meant to

represent the total uncertainty in estimated mean age at these sites. However, it provides an indication of the relative sensitivity of mean age to assumed LPM parameter values.

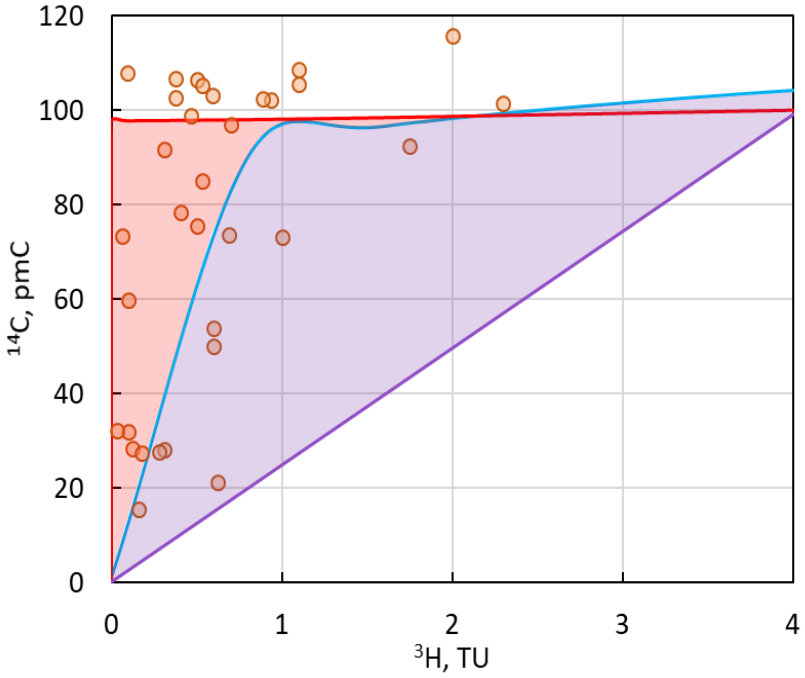

Fig S1. ^{3}H versus ^{14}C in sampled groundwater. Lines indicate LPMs (DM, *red line*; EMM, *blue line*; BMM, *purple line*). Filled areas indicate EMM-DM (*red shading*) and BMM (*purple shading*) zones. Note that this plot is an approximation for illustrative proposes. LPMs based on actual collection dates for each sample were used to estimate mean ages.

ESM References

Aeschbach-Hertig W, Peeters F, Beyerle U, Kipfer R (2000) Palaeotemperature reconstruction from noble gases in ground water taking into account equilibration with entrapped air, Nature. doi 10.1038/35016542

Aeschbach-Hertig W, El-Gamal H, Wieser M, Palcsu L (2008) Modeling excess air and degassing in groundwater by equilibrium partitioning with a gas phase, Water Resour. Res. doi 10.1029/2007WR006454.

Andrews, J.N., 1985, The isotopic composition of radiogenic helium and its use to study groundwater movement in confined aquifers, Chemical Geology. doi 10.1016/0009-2541(85)90166-4

Ballentine CJ, O'Nions RK, Oxburgh ER, Horvath F, Deak J (1991) Rare gas constraints on hydrocarbon accumulation, crustal degassing and groundwater flow in the Pannonian Basin: Earth and Planetary Sci. Let. doi 10.1016/0012-821X(91)90133-3

Crossey LJ, Fischer TB, Patchett PJ, Karlstrom KE, Hilton DR, Newell DL, Huntoon P, Reynolds AC (2006) Dissected hydrologic system at the Grand Canyon: Interaction between deeply derived fluids and plateau aquifer waters in modern springs and travertine, Geology. doi 10.1130/G22057.1

Gelhar LW, Welty C, Rehfeldt KR (1992) A critical review of data on field-scale dispersion in aquifers, Water Resour. Res. Doi 10.1029/92WR00607

Gautheron C, Moreira M (2002) Helium signature of the subcontinental lithospheric mantle, Earth and Planetary Science Letters. doi 10.1016/S0012-821X(02)00563-0.

Gibs J, Wilde FD, Heckathorn HA (2012) Use of multiparameter instruments for routine field measurements, U.S. Geological Survey Techniques of Water-Resources Investigations 09-A6.8, https://doi.org/10.3133/twri09A6.8. Cited March 30, 2020.

Han LF, Plummer LN (2013) Revision of Fontes & Garnier's model for the initial 14C content of dissolved inorganic carbon used in groundwater dating, Chem. Geo. doi 10.1016/j.chemgeo.2013.05.011

Han LF, Roller-Lutz Z, Hunjak T, Lutz HO, Maysumoto T, Aggarwal P (2017) Groundwater response to recharge in the Gacka Area, Croatia, as revealed by stable isotopes, tritium, CFCs and noble gas, Geochem. J. doi 10.2343/geochemj.2.0440

Jurgens BC, Böhlke JK, Eberts SM (2012) TracerLPM (Version 1): An Excel® workbook for interpreting groundwater age distributions from environmental tracer data, U.S. Geological Survey Techniques and Methods Report 4-F3

Kalin R.M (2000) Radiocarbon dating of groundwater systems, In: Cook PG, Herczeg AL (eds) Environmental tracers in subsurface hydrology. Kluwer Academic Publishers, Boston

Kulongski JT, Hilton DR (2011) Application of Groundwater Helium, In: Baskaran M (ed) Handbook of Environmental Isotope Geochemistry, Advances in Isotope Geochemistry. Spring-Verlag, Berlin. doi:10.1007/978-3-642-10637-8_15

Lucas LL, Unterweger MP (2000) Comprehensive review and critical evaluation of the half-life of Tritium, Journal of Research of the National Institute of Standards and Technology. doi 10.6028/jres.105.043

Mamyrin BA, Tolstikhin IN (1984) Helium Isotopes in Nature; Developments in Geochemistry, Vol. 3, Elsevier.

Manning AH, Solomon DK (2003) Using noble gases to investigate mountain-front recharge, J. Hydrol. doi 10.1016/S0022-1694(03)00043-X

Michel RL, Jurgens BJ, Young MB (2018) Tritium deposition in precipitation in the United States, 1953–2012, U.S. Geological Survey Scientific Investigations Report 2018-5086. doi 10.3133/sir20185086

National Oceanic and Atmospheric Association (2018) National Climatic Database, https://ncdc.noaa.gov/cdo-web. Cited June 15, 2018.

Radtke DB, Horowitz AJ, Gibs J, Wilde FD (2002) Raw samples, U.S. Geological Survey Techniques of Water-Resources Investigations 09-A5, https://pubs.usgs.gov/twri/twri9a5/archive/twri9a5_5.1.1-ver2.1.pdf. Cited March 30, 2020.

Reimer PJ, Bard E, Bayliss A, Beck JW, Blackwell PG, Bronk Ramsey C, Buck CE, Cheng H, Edwards RL, Friedrich M, Grootes PM, Guilderson TP, Haflidason H, Hajdas I, Hatté C, Heaton TJ, Hoffmann DL, Hogg AG, Hughen KA, Kaiser KF, Kromer B, Manning SW, Niu M, Reimer RW, Richards DA, Scott EM, Southon JR, Staff RA, Turney CSM, van der Plicht J (2013) IntCal13 and Marine13 radiocarbon age calibration curves 0–50,000 years cal BP, Radiocarbon. doi 10.2458/azu_js_rc.55.16947

Ritz GF, Collins JA (2008) pH 6.4 (ver. 2.0, October 2008), U.S. Geological Survey Techniques of Water-Resources Investigations 09- A6.4, https://doi.org/10.3133/twri09A6.4. Cited March 30, 2020.

Rounds SA (2012) Alkalinity and acid neutralizing capacity (ver. 4.0, September 2012), U.S. Geological Survey Techniques of Water-Resources Investigations 09-A6.6, https://doi.org/10.3133/twri09A6.6. Cited March 30, 2020.

Rounds SA, Wilde FD, Ritz GF (2013) Dissolved oxygen (ver. 3.0), U.S. Geological Survey Techniques of Water-Resources Investigations 9-A6.2, https://doi.org/10.3133/twri09A6.2. Cited March 30, 2020.

Skrobialowski SC (2016) Capsule- and Disk-Filter Procedure, U.S. Geological Survey Techniques of Water-Resources Investigations 09-A5.2.1, https://pubs.usgs.gov/twri/twri9a5/twri9a5_5.2.1.A.pdf. Cited March 30, 2020.

Solder JE, Beisner KR (2020) Critical evaluation of stable isotope mixing end-members for estimating groundwater recharge sources: case study from the South Rim of the Grand Canyon, Arizona, USA. Hydrogeology J. (see main article for further details)

Solomon DK (2000) ^{4}He in groundwater. In: Cook PG, Herczeg AL (eds) Environmental tracers in subsurface hydrology. Kluwer Academic Publishers, Boston

Solomon DK, Cook PG (2000) ^{3}H and ^{3}He. In: Cook PG, Herczeg AL (eds) Environmental tracers in subsurface hydrology. Kluwer Academic Publishers, Boston

Stute M, Sonntag C, Deák J, Schlosser P (1992) Helium in deep circulating groundwater in the Great Hungarian Plain: Flow dynamics and crustal and mantle helium fluxes, Geochimica et Cosmochimica Acta. doi 10.1016/0016-7037(92)90329-H

Thatcher LL, Janzer VJ, Edwards KW (1977) Methods for determination of radioactive substances in water in fluvial sediments, Techniques of Water-Resources Investigations of the U. S. Geological Survey, book 5, chap. A5, p. 79-81.

U.S. Geological Survey (2006) Collection of Water Samples (ver. 2.0), U.S. Geological Survey Techniques of Water-Resources Investigations 09-A4, https://doi.org/10.3133/twri09A4. Cited March 30, 2020.

U.S. Geological Survey (2019a) Specific conductance, U.S. Geological Survey Techniques and Methods 9-A6.3, https://doi.org/10.3133/twri09A6.3 Cited March 30, 2020.

U.S. Geological Survey (2019b) National Water Information System: U.S. Geological Survey web interface, http://dx.doi.org/10.5066/F7P55KJN. Cited June 20, 2019

Weiss RF (1968) Piggyback sampler for dissolved gas studies on sealed water samples, Deep-sea Res. 5:695-699

Wilde FD (ed) (2002) Processing of water samples, U.S. Geological Survey Techniques of Water-Resources Investigations 09-A5, https://doi.org/10.3133/twri09A5 Cited March 30, 2020.

Wilde FD (ed) (2004) Cleaning of equipment for water sampling (ver 2.0), U.S. Geological Survey Techniques of Water-Resources Investigations 9-A3, https://doi.org/10.3133/twri09A3 Cited March 30, 2020.

Wilde FD (2006) Temperature, U.S. Geological Survey Techniques of Water-Resources Investigations 09-6.1, https://doi.org/10.3133/twri09A6.1 Cited March 30, 2020.

Wilde FD, Sandstrom MW, Skrobialowski SC (2014) Selection of equipment for water sampling (ver. 3.1), U.S. Geological Survey Techniques of Water-Resources Investigations 09-A2, https://doi.org/10.3133/twri09A2 Cited March 30, 2020.